THE JOURNAL OF BIOLOGICAL CHEMISTRY VOL. 289, NO. 7, pp. 4377–4386, February 14, 2014

The Cyp2c44 Epoxygenase Regulates Epithelial Sodium Channel Activity and the Blood Pressure Responses to Increased Dietary Salt*

Received for publication, August 6, 2013, and in revised form, December 19, 2013 Published, JBC Papers in Press, December 24, 2013, DOI 10.1074/jbc.M113.508416

Jorge H. Capdevila[‡1], Nataliya Pidkovka[‡], Shaojun Mei[‡], Yan Gong[‡], John R. Falck[§], John D. Imig[¶], Raymond C. Harris[‡], and Wenhui Wang[‖]

From the [‡]Department of Medicine, Vanderbilt University, Nashville Tennessee 37232, the [§]Department of Biochemistry, University of Texas Southwestern Medical Center, Dallas, Texas 75390, the [¶]Department of Pharmacology, Medical College of Wisconsin, Milwaukee, Wisconsin 53226, and the [‖]Department of Pharmacology, New York Medical College, Valhalla, New York 10595

Background: Epoxyeicosatrienoic acids (EETs) regulate sodium excretion in the distal nephron.
Results: Lack of a Cyp2c44 epoxygenase blunts the ERK1/2-mediated inhibition of ENaC and causes salt-sensitive hypertension.
Conclusion: Cyp2c44 is the epoxygenase responsible for the synthesis of natriuretic EETs during increased salt intake.
Significance: Roles for the human CYP2C8 and CYP2C9 epoxygenases as antihypertensive therapeutic targets are proposed.

Hypertension is a major risk factor for cerebral, cardiovascular, and renal disease, and its prevalence and devastating consequences raises a need for new strategies for its early diagnosis and treatment. We show here that lack of a Cyp2c44 epoxygenase causes dietary salt-sensitive hypertension, a common form of the human disease. *Cyp2c44*(−/−) mice on normal salt diets are normotensive but become hypertensive when fed high salt. Hypertensive *Cyp2c44*(−/−) mice show a hyperactive kidney epithelial sodium channel (ENaC) and reductions in ERK1/2 and ENaC subunit phosphorylation. The demonstration that amiloride, an ENaC inhibitor, lowers the blood pressure of hypertensive *Cyp2c44*(−/−) mice identifies a role for the channel in the hypertensive phenotype of the animals. These studies: (*a*) identify an antihypertensive role for the kidney Cyp2c44 epoxygenase and for its epoxyeicosatrienoic acid (EET) metabolites in the *in vivo* control of ENaC activity and the activation of mitogenic kinase pathways; (*b*) provide evidence for a Cyp2c44 epoxygenase, EET-mediated mechanism of ENaC regulation involving an ERK1/2-catalyzed threonine phosphorylation of the channel γ subunit: and (*c*) characterize a common scientific platform that could explain the seemingly unrelated biological activities attributed to the epoxygenase metabolites in cell proliferation, angiogenesis, channel activity, and blood pressure control. It is expected that these results will serve as a basis for the development of novel strategies for the early diagnosis and treatment of hypertension and of pathophysiologies associated with dysfunctional mitogenic signaling.

Prevalence, complexity, and multiple negative medical consequences make hypertension a major health challenge, and it is widely accepted that timely diagnosis and early clinical intervention reduces its cardiovascular, cerebral, and renal complications (1, 2). However, despite intensive research, the molecular basis of prevalent forms of hypertension remain uncertain, its early diagnosis remains difficult, and its treatment remains largely symptomatic. It is expected that the identification of novel pathways/genes involved in blood pressure (BP)[2] variations (3, 4), will lead to new therapeutic targets and to improved diagnosis and prevention and thus help ameliorate the dangerous consequences of untreated chronic hypertension. Inasmuch as impairments in renal sodium transport are a feature of the most common forms of hypertension, the kidney is a target for many of the currently available antihypertensive approaches.

The kidney epithelial sodium channel (ENaC) plays important roles in the hormonal regulation of sodium reabsorption in the distal nephron and in the fine-tuning of plasma sodium levels (3–7). ENaC is composed of three subunits: α, β, and β (ENaCα, ENaCβ, and ENaCγ, respectively) (8), that mediate inward sodium transport in the apical surface of the collecting duct (CD) principal cells (7–9). The physiological importance of ENaC is illustrated by diseases in which gain or loss of function mutations in the channel are associated with hypertensive or hypotensive phenotypes, respectively (3, 10–12). Thus, Liddle syndrome, a form of severe salt-sensitive hypertension, is caused by gain of function mutations/truncations in the channel β or γ subunits (3, 10, 11), whereas loss of function mutations are associated with the hypotensive phenotype of pseudohypoaldosteronism type 1 (3, 10, 12). ENaC gating is regulated by hormones such as aldosterone, insulin, and EGF (13–16). EGF inhibits ENaC (15, 16) by mechanisms that

* This work was supported, in whole or in part, by National Institutes of Health Grants DK038226 and HL34300 (to W.-H. W.) from the U.S. Public Health Service. This work was also supported by Robert A. Welch Foundation Grant GL625910 (to J. R. F.).

Dedicated to Prof. John C. McGiff (1927–2013) in recognition of his fundamental contributions to the studies of the arachidonic acid monooxygenase pathway. He saw early on what most did not and with foresight, courage, and determination brought this field to its present status. He was a superb scientist, an excellent teacher, and an unforgettable friend and colleague.

[1] To whom correspondence should be addressed: Vanderbilt University Medical School, Medical Center North S-3223, Nashville, TN 37232. Tel.: 615-322-4968; Fax: 615-343-4704; E-mail: jorge.capdevila@vanderbilt.edu.

[2] The abbreviations used are: BP, systolic blood pressure; AA, arachidonic acid; CD, collecting duct; ENaC, epithelial sodium channel; MEK, mitogen-activated protein kinase; ERK1/2, extracellular signal regulated kinase 1 and 2; EET, epoxyeicosatrienoic acid; DHET, dihydroxyeicosatrienoic acid; NS, normal salt; HS, high salt; WT, *Cyp2c44*(+/+) genotype; KO, *Cyp2c44*(−/−) genotype; DB, *Dolichos biflorus* agglutinin.

involve an ERK1/2-catalyzed threonine phosphorylation of ENaCβ and ENaCγ (17, 18). Furthermore, in cultured mouse CD cells, 14,15-EET inhibits amiloride-sensitive sodium transport by stimulating the ERK1/2-catalyzed phosphorylation of ENaCγ (19).

The cytochrome P450 CYP2C (family 2, subfamily C) enzymes, expressed in human and rodent kidneys (20–22), catalyze the epoxidation of arachidonic acid (AA) to 5,6-, 8,9-, 11,12-, and/or 14,15-EET (20). The presence of EETs in human and rodent organs, plasma, and urine (20, 21) and the functional roles attributed to these metabolites are well documented (20–22). Measurements of sodium currents in dissected rat and mouse CDs characterized 11,12-EET as a selective inhibitor of ENaC activity (23, 24) and suggested roles for the CYP2C epoxygenases and EETs in distal sodium transport and BP control (21). However, despite extensive research, the proposal that a salt-inducible renal CYP2C epoxygenase protects against hypertension continues to be based on circumstantial evidence, and therefore, the identity and roles of the relevant epoxygenase isoform(s) in BP control remain uncertain and, at times, controversial. We report here that lack of a functional Cyp2c44 epoxygenase causes dietary salt-sensitive hypertension that is associated with increases in ENaC gating and reductions in ERK1/2 activation and in the inhibitory phosphorylation of the channel γ subunit.

EXPERIMENTAL PROCEDURES

Animal protocols were approved by the Vanderbilt University Institutional Animal Care and Use Committee. The development and genotype characterization of *Cyp2c44*(−/−) mice is published (25). Male WT and *Cyp2c44*(−/−) (KO) mice (12–20 weeks old) in isogenic *129SvE* backgrounds were used in these studies. The animals were allowed free access to water and commercial diets containing normal (NS), or high salt (HS) (0.3 and 8% (w/w) NaCl, respectively). Free fluid volume measurements were done first at 10 a.m. and then at 3 p.m. in groups of age-matched male WT and KO mice (≥5) in a Bruker Minispec mg10 nuclear magnetic resonance instrument (Bruker Biospin).

Blood Pressure Measurements—The systolic BPs of conscious 12–20-week-old mice (≥15 animals/group) were measured between 9 and 11 a.m. by means of a Micro-Renthane tapered catheter (300–500-μm outer diameter) inserted into the right carotid artery as described (26) and connected to a remote pressure sensor. 1–2 days after surgery, the animals were allowed to become familiar with the environment, and their BP was monitored for at least 40 min at an ambient temperature of 23 °C. Pressure data are averages ± S.E. calculated from ≥20 measurements/animal. Amiloride was administered in drinking water (2 mg/ml) to mice that were fed HS diets for 4 weeks. After 6 days on amiloride, systolic BPs were determined by remote telemetry by means of indwelling catheters as described (27). For the next 24 h, BPs were monitored hourly for 5 min.

Urine Analyses and Quantification of Epoxygenase Metabolites—Daily collections of urine were done between 4 p.m. and 10 a.m. in groups of age-matched WT and KO mice. Urinary sodium and potassium concentrations were measured by flame photometry. Urine creatinines were quantified by published HPLC methods (28). For analyses of epoxygenase products (EETs + DHETs), overnight urine samples were collected from groups of 3–5 adult mice in flasks containing triphenylphosphine (2–3 mg each) (29). After adding synthetic [20-$^2H_3$]-labeled 8,9-, 11,12-, and 14,15-EET (5 ng each) and [$^2H_8$]-labeled 8,9-, 11,12-, and 14,15-DHET (5 ng each) as internal standards, samples were extracted with acidified $CHCl_3$/CH_3OH (2:1) (29), the organic phases were collected and saponified (4 N KOH in 80% CH_3OH), and the samples EETs and DHETs separated by SiO_2 chromatography (using as solvents 79.5% hexane, 20% Et_2O, 0.5% HOAc for EETs and 49.5% hexane, 50% Et_2O, 0.5% HOAc for DHETs). The SiO_2-purified EETs were hydrated to DHETs (in 0.35 N HOAc). The [20-$^2H_3$]-labeled DHETs (from hydrated EETs) and [$^2H_8$]-labeled DHET isomers were resolved by ultra high pressure liquid chromatography (60 °C) on an Acquity BEH C_{18} column (1.7 μm; 1 × 100 mm) (Waters) using solvent mixtures of $CH_3COO(NH_4)$ (pH 8.5), H_2O, and CH_3CN and quantified by negative ESI/MS/MS monitoring of product ions originating from m/z 337 (m/z SRM: 127, 167, and 207 for [$^1H_1$]-labeled 8,9-, 11,2-, and 14,15-DHET), 340 (m/z SRM: 127, 167, and 207 for [$^2H_3$]-labeled 8,9-, 11,12-, and 14,15-DHET), and 345 (m/z SRM: 129, 171, and 213 for [$^2H_8$]-labeled 8,9-, 11,12-, and 14,15-DHET). Quantifications were done using isotope ratios as described (29).

Electrophysiology Studies—Cortical CDs, were microdissected from the kidneys of mice fed for 3 days diets containing 0.4 and 1.18% sodium and potassium, respectively (23, 24). These diets increased ENaC density with minimal effects on kidney Cyp2c44 expression (24). Dissected CDs were placed on an inverted microscope, superfused with Hepes-buffered NaCl (23), and cut open to expose the apical membrane. Sodium currents were recorded and digitized as described (23). Channel activity, defined as NPo, was calculated from data samples of 60 s during steady state according to: $Npo = \Sigma(t_1 + 2t_2 + \ldots it_i)$ (23) where t_I is the fractional open time spent at each observed current level. Channel conductance was calculated from currents recorded with at least three holding potentials.

Western Blot Analyses—Whole kidneys from WT or KO mice fed 4–5 weeks with NS or HS solid diets were homogenized (4 °C) in 0.1 M potassium phosphate buffer (pH 7.4) containing 0.25 M sucrose, 10 mM $Na_4P_2O_7$, 10 mM Na_3VO_4, and 1/100 volumes of protease and phosphatase 2 and 3 inhibitor cocktails (Sigma) in an T8-Ultra-Turrax (IKA, Staufen, Germany) homogenizer. After sonication (six pulses, power 4) (Ultrasonic Homogenizer 4710; Cole Parmer Instruments), the homogenates were centrifuged for 15 min at 5,000 and 10,000 × g. Membrane fractions were collected from 10,000 × g supernatants by a 60-min centrifugation at 100,000 × g, suspended in fresh homogenization buffer, and used within the next 4 h. Western blot analyses of kidney homogenates or membranes were performed by standard electrophoretic/blotting techniques using the following rabbit peptide antibodies: anti-Cyp2c44 from GenScript; anti-phospho-ERK1/2 (Tyr-202/204), anti-phosphothreonine from Cell Signaling Technologies; anti-ERK1/2 and anti-ENaCγ from Santa Cruz Biotechnology; and anti-β-actin from Sigma. Control experiments showed that only lot 16 of the anti-phosphothreonine antibod-

ies purchased from Cell Signaling Technologies recognized protein(s) with the electrophoretic mobility reported for the native channel γ subunit (75–80 kDa) (30) and immunoreactive toward anti-ENaCγ antibodies. Immunoreactive proteins were detected with an Immobilon Western chemiluminescent HRP substrate kit (Millipore) and quantified by x-ray silver grain densitometry.

Immunofluorescence Imaging—Paraffin sections (5 μ each) from the kidneys of WT and KO mice were perfused *in situ* with 40 mM sodium phosphate buffer (pH 7.4) containing 4% formaldehyde, 0.1 M NaCl, 50 mM NaF, 0.5 mM Na_3VO_3, 30 mM $Na_4P_2O_7$, and 0.1% HOAc; fixed in paraffin; and exposed to white light for 48–72 h to reduced autofluorescence. After paraffin removal, hydration, and microwave antigen retrieval in 1× Citra Buffer (BioGenex), the sections were blocked in 10% goat serum; incubated with biotinylated *Dolichos biflorus* agglutinin (DB) (Vector Labs), a CD marker (31), rabbit anti-phosphothreonine antibodies (Cell Signaling Technologies, lot 16); and then exposed to fluorescein isothiocyanate-conjugated streptavidin (GE Healthcare) and rhodamine-conjugated goat anti-rabbit IgGs (Jackson ImmunoResearch Laboratories).

Statistical Analysis—The data sets from paired/unpaired groups were analyzed for statistical significance using a two-tailed Student's *t* test (Excel). *Error bars* represent S.E. *p* values of ≤0.05 were considered statistically significant.

RESULTS

The murine Cyp2c44 epoxygenase and its rat homologue, CYP2C23 (polypeptides 23 and 44), share 88% amino acid sequence identity (20, 32) and metabolize AA to predominantly 11,12- and 14,15-EET (20, 32). Roles for these enzymes in BP regulation were indicated by the demonstration that their kidney expression was dietary salt-sensitive (21, 26, 33) and that hypertensive salt-sensitive Dahl rats showed reduced renal CYP2C23 epoxygenase expression and EET biosynthesis (33). However, the complexity of the Dahl rat salt-sensitive genotype precluded unequivocal evaluations of roles for the *CYP2C23* gene in salt-sensitive hypertension (33). Therefore, to define the role of the Cyp2c epoxygenases in BP regulation, mice carrying a disrupted *Cyp2c44*(−/−) gene were generated from an ES cell line (Ommibank clone OST85045) (Lexicon Genetics Inc.) and characterized as reported (25). The KO mice developed normally and lacked outward symptoms of disease or organ malformation. Light microscopy of paraffin sections and measurements of plasma creatinine (28) showed that disruption of the *Cyp2c44* gene had no obvious effects on kidney morphology or gross function (plasma creatinine of 57 ± 5 and 53 ± 2 and of 58 ± 3 and 56 ± 4 μg/dl for WT and KO mice fed NS or HS diets, respectively; $n \geq 10$ animals). Furthermore, only small differences in creatinine excretion were observed between KO mice on NS or HS diets (23 ± 1 and 27 ± 1 mg/18 h urine collections for KO on NS and HS diets, respectively; $p = 0.04$; $n \geq 31$).

The Cyp2c44 Epoxygenase and the Pressure Responses to Increased Dietary Salt Intake—Roles for the Cyp2c44 epoxygenase in the regulation of systemic BPs were identified after feeding NS or HS diets to WT and KO mice. As shown in Fig. 1*A*, small but significant differences were observed in the systolic

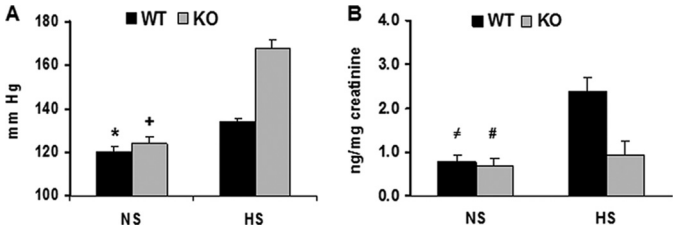

FIGURE 1. **Lack of a functional Cyp2c44 epoxygenase causes dietary salt-sensitive hypertension.** Male WT (*black bars*) and KO (*gray bars*) mice were fed NS or HS solid diets (containing 0.3 or 8% NaCl (w/w), respectively), and after 4–5 weeks, their systolic BP (*A*) and urinary levels of total epoxygenase metabolites (EETs + DHETs) (*B*) were determined as described under "Experimental Procedures." *A*, values are averages ± S.E. of ≥25 measurements done in groups of at least 15 mice each for WT on NS or HS and KO on NS and 25 KO mice on HS. *, significantly different from WT on HS ($p < 10^{-72}$) and KO on NS ($p < 10^{-8}$). +, significantly different from KO on HS ($p < 10^{-170}$). *B*, values are averages ± S.E. calculated from groups of at least five mice. ≠, significantly different from WT on HS ($p < 10^{-5}$). #, significantly different from WT on HS ($p < 10^{-6}$). The differences between WT and KO mice fed NS and from KO mice fed NS or HS were not significant ($p > 0.05$).

BP of WT and KO mice on NS (120 ± 3 and 124 ± 3 mm Hg, for WT and KO, respectively). After 4 weeks on HS diets, WT mice showed small increases in systolic BP (to 134 ± 2 mm Hg) (Fig. 1*A*), whereas under similar conditions, the KO animals became severely hypertensive (168 ± 4 mm Hg) (Fig. 1*A*). Quantifications of total urinary epoxygenase metabolites (EETs + DHETs) showed that HS increased their levels in WT mice (from 0.78 ± 0.17 to 2.38 ± 0.33 ng/mg of creatinine) (Fig. 1*B*), and the animals remained normotensive (Fig. 1*A*), whereas in contrast, KO mice were unable to do so and became hypertensive (Fig. 1, *A* and *B*). As seen in Fig. 1*B*, KO mice on HS diets show basal levels of urinary epoxygenase metabolites similar to those of WT and KO mice on NS, suggesting that they are likely generated by non-salt-sensitive kidney epoxygenases such as Cyp2c29 and/or Cyp2c38 (34). Analyses of the combine regioisomeric composition of the EETs + DHETs present in urine, as estimates of renal 11,12- and 14,15-epoxygenase activities, indicated that: (*a*) regardless of dietary salt intake or *Cyp2c44* genotype, the major urinary metabolites result from epoxidation at the AA 14,15-olefin and, to a lesser extent, 11,12-epoxygenation (Table 1); (*b*) the levels and the isomeric composition of the EET + DHTs present in the urines of WT and KO mice on NS were similar (Table 1); (*c*) feeding HS diets to WT mice increases by approximately 3-fold the urine concentrations of 11,12- and 14,15-epoxygenase derived metabolites, but it does not significantly alter their isomeric composition (Table 1); (*d*) compared with WT animals on HS, KO mice fed HS show 5.6- and 2.1-fold lower urinary levels of the Cyp2c44 derived 11,12- and 14,15-epoxygenase products, respectively (Table 1); and (*e*) only low levels of 8,9-epoxygenase metabolites are present in urines from WT and KO mice, and their concentrations are not significantly altered by changes in salt intake and/or *Cyp2c44* gene disruption (not shown).

In summary, the above studies show that failure to up-regulate the Cyp2c44 epoxygenase (in particular, 11,12-EET biosynthesis) in response to increases in salt intake (Fig. 1*B* and Table 1) raises BP and causes hypertension (Fig. 1*A*). Similar salt effects have been reported for Dahl rats in which only salt-resistant animals induce renal EET biosynthesis during salt loading and remain normotensive (33). Taken together, these

TABLE 1

Epoxygenase metabolites present in the urine of WT and Cyp2c44 KO mice

The sums of 11,12-EET and 11,12-DHET and of 14,15-EET and 14,15-DHET present in the urines of WT and *Cyp2c44* KO mice fed diets containing 0.3% (NS) or 8% (HS) NaCl for 4–5 weeks were quantified by UPLC/MS/MS as described under "Experimental Procedures." The data shown are the sums of metabolites (EET + DHET) resulting from epoxidation at the AA 11,12- and 14,15-olefins (in ng/mg of creatinine), as well as their distribution percentages. The values are averages ± S.E. calculated from at least 10 different experiments. The differences in distribution of 11,12- or 14,15-epoxygenase products between WT mice on NS or HS or between WT and KO mice on NS were not significant ($p > 0.05$).

	11,12-Epoxygenase		14,15-Epoxygenase	
Mice/diet	ng/mg	% of total	ng/mg	% of total
WT NS[a]	0.19 ± 0.02	24 ± 2	0.57 ± 0.02	73 ± 3
KO NS[b]	0.19 ± 0.02	27 ± 3	0.46 ± 0.03	67 ± 5
WT HS[c]	0.62 ± 0.07	26 ± 3	1.71 ± 0. 71	72 ± 3
KO HS	0.11 ± 0.01	12 ± 1	0.80 ± 0.09	86 ± 1

[a] Significant differences were observed between the distribution of 11,12-epoxygenase metabolites ($p = 0.0002$) and 14,15-epoxygenase ($p = 0.0002$) *versus* KO HS.
[b] Significant differences were observed between the distribution of 11,12-epoxygenase metabolites ($p = 10^{-5}$) and 14,15-epoxygenase ($p = 0.0006$) *versus* KO HS.
[c] Significant differences were observed between the distribution of 11,12-epoxygenase metabolites ($p = 10^{-4}$) and 14,15-epoxygenase ($p = 0.0005$) *versus* KO HS.

TABLE 2

Dietary salt induced changes in the weight and urine parameters of WT and Cyp2c44KO mice

Body weights, volumes of urine collected between 4:00 p.m. and 10:00 a.m., and spot urine sodium and potassium concentrations were measured from groups of WT and *Cyp2c44*(−/−) (KO) mice fed NS or HS diets for 4–5 weeks. Shown are averages ± S.E., calculated from measurements done on groups of ≥35 (body weight), ≥20 (urine volume), and ≥60 (sodium and potassium concentrations) WT and KO mice on NS or HS diets. Significant differences are indicated in the footnotes; no additional significant differences between the two genotypes were detected in body weights, urine volumes, and sodium or potassium concentrations ($p > 0.05$).

		Urine		
Mice/diet	Weight	Volume	Sodium	Potassium
	g	*ml*	*mM*	*mM*
WT NS[a]	28.8 ± 0.3	1.0 ± 0.1	173 ± 9	307 ± 14
KO NS[b]	27.6 ± 0.3	1.1 ± 0.1	153 ± 10	254 ± 24
WT HS[c]	29.1 ± 0.3	4.2 ± 0.3	478 ± 21	53 ± 3
KO HS	29.0 ± 0.3	5.4 ± 0.4	414 ± 19	43 ± 3

[a] Significant differences were observed between the weights ($p = 0.008$ *versus* KO NS), the urine volumes ($p = 10^{-12}$ *versus* WT HS), the urine sodium concentrations ($p = 10^{-29}$ *versus* WT HS), and the urine potassium concentrations ($p = 10^{-30}$ and 0.04, respectively, *versus* WT HS and KO NS).
[b] Significant differences were observed between the weights ($p = 0.002$ *versus* KO HS), the urine volumes ($p = 10^{-19}$ *versus* KO HS), the urine sodium concentrations ($p = 10^{-23}$ *versus* KO HS), and the urine potassium concentrations (p 10^{-13}, respectively, *versus* KO HS).
[c] Significant differences were observed between the urine volumes ($p = 0.01$ *versus* KO HS) and the urine sodium concentrations ($p = 0.02$ *versus* KO HS).

TABLE 3

Concentrations of sodium and potassium present in the plasmas of WT and Cyp2c44 KO mice fed normal or high salt diets

The concentrations of sodium and potassium present in plasma samples from WT and *Cyp2c44*(−/−) (KO) mice fed solid diets containing either 0.3% NaCl (NS) or 8% NaCl (HS) diets for 4–5 weeks were determined by flame photometry. Shown are averages ±S.E. calculated from plasmas isolated from groups of at least 19 mice each. Significant differences are indicated in the footnotes; no significant differences in sodium concentrations were detected between WT and KO mice fed either NS or HS diets ($p > 0.05$).

	Plasma	
Mice/diet	Sodium	Potassium
	mM	
WT NS[a]	141 ± 2	9.6 ± 0.5
KO NS[b]	143 ± 1	10.8 ± 0.2
WT HS[c]	144 ± 2	8.2 ± 0.2
KO HS	144 ± 2	8.4 ± 0.6

[a] Significant differences in potassium concentrations were observed ($p = 0.02$ *versus* WT HS).
[b] Significant differences in potassium concentrations were observed ($p = 0.03$ *versus* KO HS).
[c] Significant differences in potassium concentrations were observed ($p = 0.007$ *versus* KO NS).

studies: (*a*) show that the Cyp2c44 epoxygenase mediates dietary HS-induced increases in renal EET biosynthesis; (*b*) demonstrate that a dysfunctional *Cyp2c44* gene causes salt-sensitive increases in systemic BP; and (*c*) identify the Cyp2c44 epoxygenase as a dietary salt-sensitive antihypertensive enzyme and point to roles for its EET metabolites in systemic BP control (21, 35). Of interest, the pressure responses of KO mice to dietary salt are similar to those seen in a mouse model of Liddle syndrome with a hyperactive ENaC because of a deletion in the C terminus of ENaCβ (6).

The weights of KO mice fed NS were lower than those of comparable WT animals on NS or HS diets (Table 2), and although a HS diet had nonsignificant effects on the weight of WT mice, it increased that of KO mice by 5% (Table 2). Nuclear magnetic resonance measurements showed that free fluid volumes in KO mice fed HS were higher than those of matched WT controls (1.3 ± 0.1 and 1.1 ± 0.1, as a percentage of body weight, respectively) (WT *versus* KO, $p \leq 0.03$; $n = 5$). These effects of HS on body weight and free fluid volume suggested that fluid retention may be a component of salt-sensitive hypertensive phenotype of KO mice. Measurements of urine volumes collected during 18-h periods showed significant volume differences between WT and KO mice only when the animals were fed HS (Table 2). Spot urine analyses revealed *Cyp2c44* genotype-determined significant differences in the concentrations of: (*a*) potassium in mice fed NS or HS diets (Table 2) and (*b*) sodium in animals fed a HS diets (Table 2). However, these *Cyp2c44* genotype-determined differences in urinary sodium and potassium concentrations (Table 2) were minimized when their total excretion levels were calculated for 18-h collection periods. The observation that WT and KO mice on a HS diet excrete similar amounts of sodium is similar to what has been reported for Dahl S and R rats on HS mice (36) or during severe hypervolaemia (37), as well as for subsets of human hypertension (38). Finally, analyses of plasma sodium and potassium concentrations showed that, regardless of dietary salt intake, sodium levels were similar for WT and KO mice (Table 3), whereas those of potassium were lower in HS fed mice, regardless of genotype (Table 3).

The Salt-sensitive Hypertensive Phenotype of Cyp2c44 KO Mice Is Associated with a Dysfunctional ENaC—Electrophysiology studies in freshly dissected cortical CDs showed that, compared with WT, KO mice have increased ENaC-mediated inward sodium currents and an hyperactive channel (Fig. 2, *A* and *B*), a phenotype similar to that seen in Liddle syndrome patients (3, 10, 11). Moreover, although AA, the Cyp2c44 epoxygenase substrate, inhibited ENaC gating in the CDs of WT animals, it had no significant effects on those from KO mice lacking the epoxygenase (Fig. 2, *A* and *B*). Roles for the Cyp2c44 epoxygenase in ENaC regulation were demonstrated by the observation that exogenously added 11,12-EET inhibited ENaC gating in CDs of KO mice and thus reversed the KO phenotype (Fig. 2*B*). These results are summarized in Fig. 2*C* in which channel gating is expressed as a percentage of normalized activity (*i.e.*, channel numbers multiplied by their open

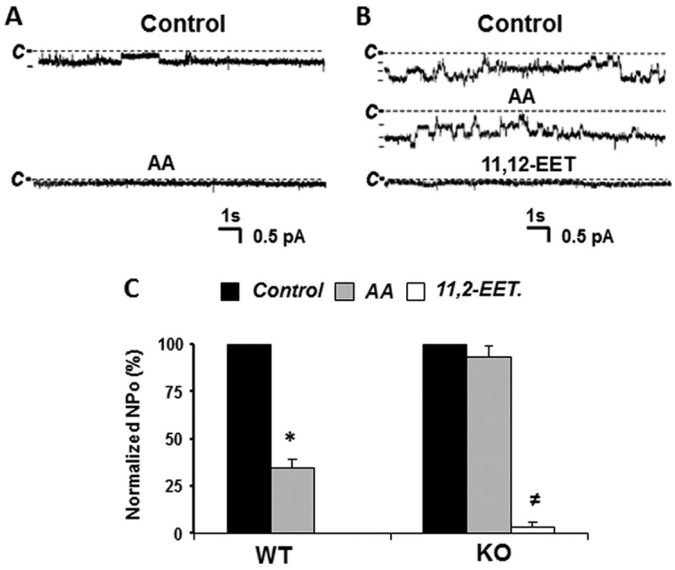

FIGURE 2. **ENaC is hyperactive in the collecting ducts of Cyp2c44 KO mice.** Sodium currents were determined in cell attached patches as described (23, 24). *A* and *B*, patch clamp recordings of sodium currents in microdissected CDs from WT (*A*) and KO (*B*) mice. Channel closed levels are indicated by *C*, and *dotted lines* indicate current levels for a fully closed channel. *Horizontal* and *vertical short bars* indicate time in seconds and currents in pA, respectively. *C*, normalized ENaC activity (NPo) under control conditions (*black bars*), or in the presence of either 10 μM AA (*gray bars*) or 0.2 μM 11,12-EET (*white bar*). The values (as a percentage of control activity) are averages ± S.E. calculated from at least five experiments. *, significantly different from controls ($p < 0.01$). ≠, significantly different from controls ($p < 0.001$).

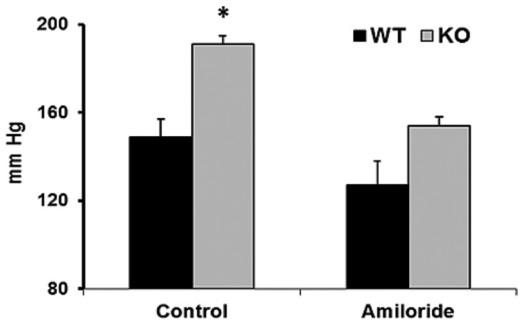

FIGURE 3. **Amiloride lowers the blood pressures of hypertensive Cyp2c44 KO mice.** The systolic BPs of male WT (*black bars*) and KO (*gray bars*) mice (five and seven animals, respectively) fed a HS diets for 4 weeks were calculated from 24-h remote telemetry measurements (27). Shown are average values ± S.E. obtained after 5 days of a daily administration of a 2 mg/ml amiloride solution as drinking water. *, significantly different from amiloride-treated KO mice ($p < 0.01$). The differences between WT mice on amiloride or water or between the WT and KO animals on amiloride were not significant ($p > 0.05$).

probabilities). Overall, these studies identify the Cyp2c44 epoxygenase and 11,12-EET as regulators of ENaC activity and distal sodium reabsorption, and provide a functional link between a hyperactive ENaC and the hypertensive phenotype of salt-loaded KO mice. In summary, disruption of the *Cyp2c44* gene results in a CD epoxygenase functional knock-out, which recapitulates many of the functional properties attributed to these enzymes and their products (20–22).

Amiloride Lowers the Blood Pressures of Hypertensive Cyp2c44 KO Mice—Amiloride inhibits ENaC gating and promotes sodium excretion and potassium sparing (8). To determine the contribution of ENaC dysfunction to the hypertensive phenotype of KO mice, the BPs of WT and KO animals on HS salt diets were monitored by remote telemetry before and after the daily administration of amiloride. After 6 days on amiloride, the BPs of hypertensive KO mice were reduced to levels comparable to those of untreated WT mice (from 191 ± 4 to 154 ± 6 mm of Hg, for untreated and amiloride-treated KO mice, respectively (Fig. 3). Amiloride also lowered the BPs of salt-loaded WT mice (from 148 ± 8 to 127 ± 11 mm of Hg for untreated and amiloride treats WT mice, respectively), and although its effects were variable and not statistically significant ($p > 0.05$) (Fig. 3), they are likely associated with known effects of amiloride in basal, nonstimulated, ENaC activity (26, 35) and its attendant effects in sodium excretion, and/or indirect, compensatory, effects on non-ENaC kidney epithelial channels/transporters known to participate in sodium excretion. However, the strong pressure lowering effects of amiloride on *Cyp2c44* KO mice fed HS diets corroborates the role played by ENaC in their salt-sensitive phenotype. Taken together, these results identify roles for: (*a*) ENaC dysfunction as a major component of the hypertensive phenotype of KO mice and (*b*) the Cyp2c44 epoxygenase and the EETs in the *in vivo* regulation of ENaC gating and distal sodium excretion (39). Of note, although the pressure differentials between salt-loaded WT and KO mice were similar (35–40 mm Hg) whether measured by ambulatory catheters (Fig. 1*A*) or remote telemetry methods (Fig. 3), telemetry yielded consistently higher pressure values for both animals, perhaps reflecting the fact that telemetry data were calculated from hourly measurements performed during 24-h cycles, including night time.

Mechanisms of EET-mediated Regulation of ENaC Gating—The inhibition of ENaC by EGF was shown to involve an ERK1/2-catalyzed phosphorylation of threonine targets in the channel β and γ subunits (17). Studies in cultured mouse CD cells showed that: (*a*) 11,12- and 14,15-EET inhibit ENaC gating (40) and (*b*) 14,15-EET inhibited transcellular amiloride-sensitive sodium transport by an ERK1/2-catalyzed threonine phosphorylation of ENaCβ and ENaCγ (19). Studies in freshly dissected CDs identified 14,15-EET as a less effective ENaC inhibitor than 11,12-EET (23, 24), suggesting that cultured CDs cells (19, 40) are either intrinsically less EET regioselective or metabolize/inactivate 14,15-EET at substantially lower rates than dissected CDs (20, 22). Importantly, the demonstration that cetuximab, an inhibitor of EGF receptor binding and signaling, causes hypertension in mice and reduces ENaCγ threonine phosphorylation (19) lends support to a proposal that the EGF-mediated ERK1/2-catalyzed phosphorylation of ENaC subunits plays an *in vivo* role in the control of the channel activity and BP (19). Based on these and published studies (15–19, 41, 42), it was hypothesized that: (*a*) EGF and Cyp2c44 epoxygenase-derived EETs regulated ENaC activity by common, ERK1/2-mediated mechanisms and (*b*) impairments in ERK1/2 activation and ENaC phosphorylation contribute to the hypertensive phenotype of *Cyp2c44* KO mice.

To explore the *in vivo* roles played by the Cyp2c44 epoxygenase in ERK1/2 activation, we probed Western blots of kidney homogenates from WT and KO mice fed NS or HS diets with anti-ERK1/2 and anti-phospho-ERK1/2 antibodies. As shown in Fig. 4 (*A* and *D*), the kidneys of WT and KO mice on NS

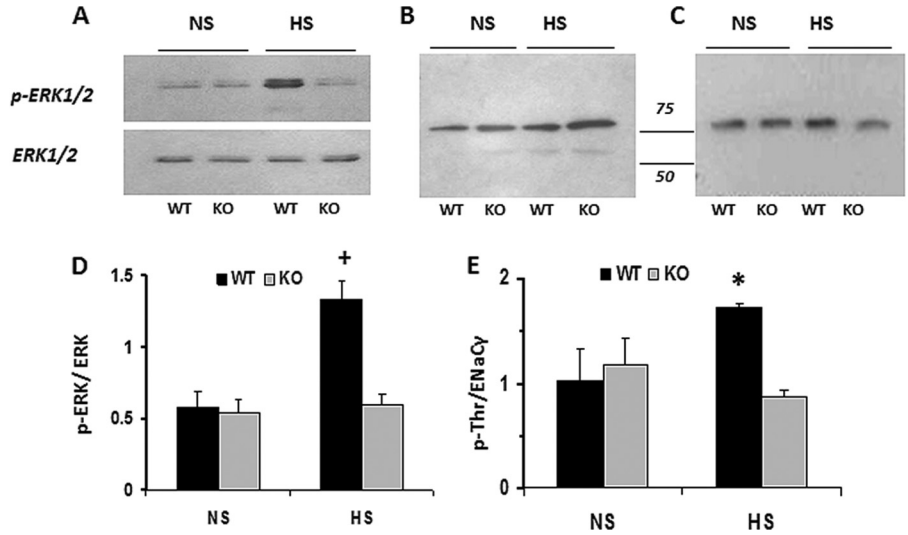

FIGURE 4. **ERK1/2 and ENaCγ phosphorylation are decreased in the kidneys of salt-loaded Cyp2c44 KO.** *A–C*, kidneys from WT and KO mice fed NS or HS diets for 4 weeks were collected from groups of three different mice each, mixed, homogenized, fractionated as described under "Experimental Procedures," and submitted to Western blot analyses using homogenates and anti-ERK1/2 (10 μg of protein/well) or anti-phospho-ERK1/2 antibodies (20 μg of protein/well) (*A*), membrane fractions (40–60 μg of protein/well) and anti-ENaCγ antibodies (*B*), and membrane fractions (30–40 μg of protein/well) and anti-phosphothreonine antibodies (*C*). Shown are proteins immunoreactive toward anti-phospho-ERK1/2 (*top panel*) or anti-ERK1/2 (*bottom panel*) antibodies (*A*), anti-ENaCγ antibodies (*B*), and anti-phosphothreonine antibodies (*C*). Sample loadings for *A* and *C* were adjusted based on the samples immunoreactivity toward anti-ERK1/2 and -ENaCγ antibodies, respectively. *B* and *C* show relative mobilities for 75- and 50-kDa proteins standards. *D*, quantification of immunoreactive proteins by silver grain densitometry of x-ray films originating from Western blots of anti-ERK1/2 and anti-phospho-ERK1/2 antibodies. Shown are averages of ERK1/2 normalized levels of phospho-ERK1/2 expression calculated from 14 different experiments ± S.E. +, significantly different from WT NS ($p < 0.0003$), KO NS ($p < 0.00004$), and KO HS ($p < 0.0001$). The differences between WT NS and KO NS or KO HS and between KO NS and KO HS were not significant ($p \geq 0.05$). *E*, quantification of immunoreactive proteins by silver grain densitometry of x-ray films originating from Western blots of anti-ENaCγ and anti-phosphothreonine antibodies. Shown are averages of ENaCγ normalized levels of phosphothreonine expression calculated from 14 different experiments ± S.E. *, significantly different from KO HS ($p < 0.02$). The differences between WT NS and KO NS or KO HS and between KO NS and KO HS were not significant ($p \geq 0.05$).

contained similar levels of phosphorylated ERK1/2. Feeding a HS diet increases ERK1/2 activation in the kidneys of WT mice, but it fails to do so in KO animals (Fig. 4, *A* and *D*). To determine whether *Cyp2c44* genotype differences in ERK1/2 activation led to changes in the levels of anti-phosphothreonine and anti-ENaCγ immunoreactive proteins with the electrophoretic mobility of native ENaCγ (30), membranes from the kidneys of WT and KO mice fed NS or HS were analyzed by Western blot using anti-ENaCγ and anti-phosphothreonine antibodies (see "Experimental Procedures" for details), and sample loadings were adjusted to yield similar levels of anti-ENaCγ immunoreactive proteins. As seen in Fig. 4 (*B* and *C*), the kidneys of WT and KO mice on NS showed similar levels of anti-phosphothreonine immunoreactive proteins (Fig. 4, *B* and *C*). In contrast, compared with salt-loaded normotensive WT mice, hypertensive KO mice fed HS showed lower amounts of anti-phosphothreonine immunoreactive proteins (Fig. 4*C*), even when electrophoresed in the presence of slightly higher levels of anti-ENaCγ immunoreactive proteins as seen in Fig. 4*B*. Quantifications of Western blot data by densitometry showed that, when normalized based on the samples contents of anti-ENaCγ immunoreactive proteins, the kidney levels of anti-phosphothreonine immunoreactive proteins with mobilities similar to native ENaCγ (30) are similar for normotensive WT and KO mice on NS and that although a HS diet increases them in normotensive WT mice, it fails to do so in hypertensive KO mice (Fig. 4*E*).

ENaC is expressed along aldosterone-sensitive segments of the distal nephron and, in particular, in cortical and medullary CDs where ENaC-mediated sodium reabsorption predominates (3, 7, 13). To determine whether the CD was a target of HS-induced, *Cyp2c44* genotype-dependent changes in ENaCγ threonine phosphorylation (Fig. 4, *C* and *E*), paraffin-fixed sections from the kidneys of WT and KO mice fed either NS or HS diets were exposed sequentially to biotinylated DB, a CD marker (31), rabbit anti-phosphothreonine antibodies, fluorescein isothiocyanate-conjugated streptavidin, and rhodamine-conjugated goat anti-rabbit IgGs, as described under "Experimental Procedures." Fluorescence microscopy of the stained sections showed the presence and co-localization in the kidneys of WT mice on NS or HS and of KO mice on NS of green and red emissions originating from the CD marker and the anti-phosphothreonine immunoreactive proteins, respectively (Fig. 5, *A* and *top panels* in *B*, and Fig. 6). In contrast, images of kidneys from hypertensive salt-loaded KO mice revealed, in agreement with the Western blot data (Fig. 4, *C* and *E*), marked reductions in the overall abundance of anti-phosphothreonine immunoreactive proteins in their CDs, whether the sections were analyzed at high (Fig. 5*B*, *bottom row*) or medium magnification (Fig. 6). Furthermore, the kidneys of normotensive WT and KO mice fed NS diets show more or less similar levels of anti-phosphothreonine reactive material in their CDs (Figs. 5 and 6). As mentioned, the anti-phosphothreonine antibodies used in these experiments recognized protein(s) immunoreactive toward ENaCγ antibodies (Fig. 4, *B* and *C*). Control experiments showed that preincubation of the anti-phosphothreonine antibodies with a synthetic threonine-phosphorylated peptide coding for the target threonine and flanking residues in ENaCγ (PEAPVPG-(*T*-p)-PPPRYN (17, 30) blunted, selectively, the red fluorescence emissions associated with immuno-

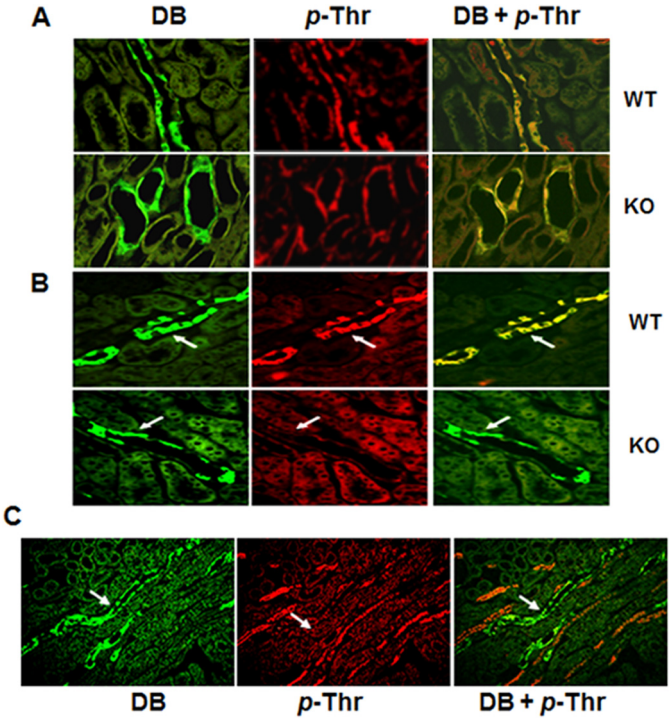

FIGURE 5. **The collecting ducts of Cyp2c44 KO mice show reduced anti-phosphothreonine antibody associated immunofluorescence.** *A* and *B*, paraffin-embedded kidney sections from mice fed NS (*A*) or HS (*B*) diets for 4 weeks were exposed to DB and rabbit anti-phosphothreonine antibodies (*p-Thr*) and then to fluorescein isothiocyanate-conjugated streptavidin and rhodamine-conjugated goat anti-rabbit IgGs as described under "Experimental Procedures." Shown are 400× microscope images of *green* (DB), *red* (*p*-Thr), and overlay fluorescence (DB + *p*-Thr) (*left*, *center*, and *right panels*, respectively) emissions and showing the presence of DB positive (*green*) CDs and anti-phosphothreonine positive (*red*) fluorescence in the CDs of WT and KO mice on NS and WT mice on HS diets (*A* and *B*, *top panel*); the absence of anti-phosphothreonine immunoreactive material in the CDs of KO mice on HS diets (Fig. 5*B*, *bottom panel*); and the co-localization *green* and *red* emissions only in kidney sections from WT and KO animals on NS and WT mice on HS (Fig. 5*A*, and Fig. 5*B* top frame). The *white arrows* in *B* point to DB positive CDs and to the presence of anti-phosphothreonine positive CDs in sections from HS WT mice and their absence in sections from hypertensive HS KO animals. *C*, samples of anti-phosphothreonine IgGs (0.3 μg of protein each) were incubated with a synthetic ENaC γ peptide (30 μg) containing the reported phosphorylated threonine (17, 18) and flanking residues (see "Experimental Procedures" for details). After 5 h at 4 °C, paraffin-embedded kidney sections from WT mice on NS were exposed first to DB and then to the anti-phosphothreonine antibodies incubated with the ENaCγ threonine-phosphorylated peptide, and the immunofluorescence analyses were continued as above. Shown are 200× microscope images of *green* (DB), *red* (*p*-Thr), and overlay fluorescence (DB + *p*-Thr) (*left*, *center*, and *right panels*, respectively) emissions and showing a lack of red fluorescence emissions in DB-positive (*green*) CDs and its presence in non-CD tubular segments. *White arrows* point to DB positive and anti-phosphothreonine negative tubular segments.

reactive material in biotinylated *Dolichos biflorus* agglutinin (DB)-positive segments of the nephron (Fig. 5*C*).

Finally, notwithstanding lack of physical evidence to corroborate the ENaCγ nature of the anti-ENaCγ immunoreactive materials mentioned above, the Western blot and immunofluorescence data in Figs. 4–6, as well as published studies (19), support a role for the MEK/ERK1/2 pathway as the catalyst of the EGF/Cyp2c44 epoxygenase mediated inhibitory phosphorylation of ENaCγ and point to roles for the Cyp2c44 epoxygenase in: (*a*) controlling the effects of dietary HS intake on kidney ERK1/2 phosphorylation and (*b*) the inhibitory, ERK1/2-mediated phosphorylation of ENaCγ. Finally, poor signal to noise ratios precluded meaningful analyses of dietary salt and/or *Cyp2c44* genotype on ENaCβ phosphorylation with commercially available anti-ENaCβ antibodies.

DISCUSSION

Salt-sensitive hypertension, a common form of the disease in the Western world, is associated with alterations in renal sodium transport leading to sodium retention and compensatory increases in extracellular fluid volume. The CD participates in the fine tuning of plasma sodium levels, and sodium reabsorption by ENaC is a rate-limiting step in this important function (3, 7). The report that luminal EETs inhibited sodium reabsorption in perfused rabbit CDs was the first indication of roles for these lipids in distal sodium transport (39). Subsequently, the demonstration that: (*a*) the kidney expression of rat CYP2C23 and mouse Cyp2c44 epoxygenases was salt-sensitive (21, 26, 33), (*b*) epoxygenase inhibition caused salt-sensitive hypertension (21, 33), and (*c*) hypertensive Dahl salt-sensitive rats show reduced kidney epoxygenase activity (21, 33) suggested antihypertensive roles for these enzymes and their metabolites (21). Evidence that: (*a*) 11,12-EET, but not 11,12-DHET, inhibited ENaC gating in dissected CDs (23, 24, 26, 35); (*b*) 11,12- and 14,15-EET inhibited ENaC gating in cultured CD cells (40); (*c*) BP was associated with renal Cyp2c44 expression (26); and (*d*) during high potassium intake the Cyp2c44 epoxygenase suppressed sodium reabsorption in the aldosterone-sensitive nephron (35), lent further support to proposals of roles for the CYP2C epoxygenases in the biosynthesis of antihypertensive EETs. The present characterization of salt-loaded KO mice as hypertensive provides now unequivocal evidence that the Cyp2c44 epoxygenase plays a key physiological role in the control of distal sodium excretion and systemic BP and that alterations in its activity and/or expression causes dietary salt-sensitive hypertension. Moreover, the demonstration that: (*a*) *Cyp2c44* KO mice show a constitutively hyperactive ENaC that is inactivated by 11,12-EET but not its precursor AA and (*b*) that amiloride normalizes the BP of salt-loaded *Cyp2c44* KO mice points to roles for the epoxygenase and its EET metabolites as endogenous regulators of ENaC gating and natriuretic agents. In summary, the hypertensive phenotype of *Cyp2c44* KO mice is reminiscent of a component of what is seen in patients of Liddle syndrome with a hyperactive kidney CD ENaC (3, 10, 11).

Multiple mechanisms are known to participate in the regulation of ENaC activity, including limited proteolysis (30, 43, 44), hormonal mediated effects on translocation and membrane assembly (9, 13, 45, 46), a serum and glucocorticoid-regulated kinase (SGK-1)-mediated phosphorylation of Nedd4–2 leading to reduced ubiquitination, retrieval and degradation (17, 18, 47, 48), as well as negative and positive hormonal effects mediated by protein kinases including ERK1/2, protein kinases A and C, and phosphatidylinositol 3-kinase, among others (14–19, 47–49). Added to the above is the present identification of the Cyp2c44 epoxygenase and its EET metabolites as a new class of *in vivo* regulators of ENaC activity.

The involvement of an ERK1/2-catalyzed threonine phosphorylation of the ENaC β and γ subunits in the inhibition of amiloride-sensitive sodium transport by 14,15-EET is pub-

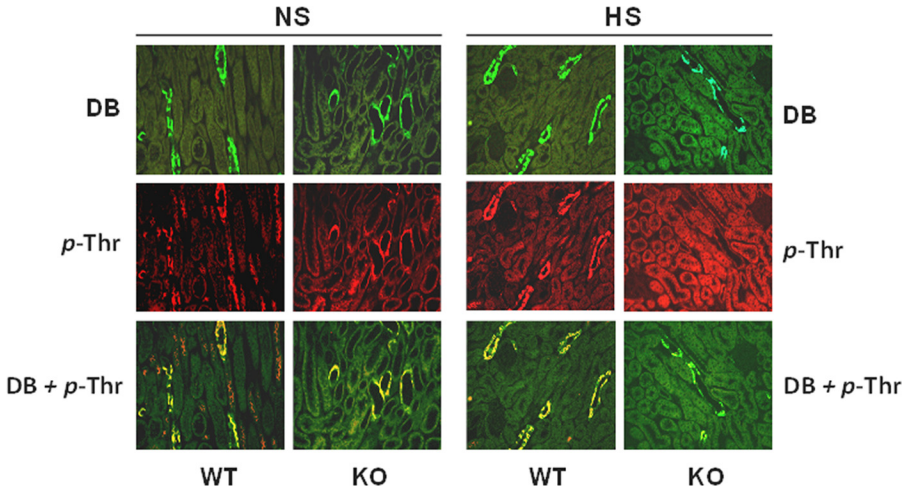

FIGURE 6. **Medium resolution immunofluorescence images of kidney sections from WT and Cyp2c44(−/−) (KO) mice fed normal or high salt diets.** Paraffin sections from the kidneys of adult male WT and KO mice fed NS or HS diets for 4–5 weeks were co-stained with anti-phosphothreonine antibodies (*red*) and *D. biflorus* agglutinin (*green*), a collecting duct marker. Shown are 200× microscope images of *green* (DB), *red* (*p*-Thr), and overlay *green* and *red* (DB + *p*-Thr) emission fluorescence illustrating the relative abundance of anti-phosphothreonine immunoreactive proteins in the collecting ducts of WT and KO mice fed NS and WT mice fed HS diets (containing 0.3 or 8% NaCl, respectively) for 4 weeks and their scarcity in the collecting ducts of KO animals on a HS diet.

lished (19), as is the demonstration that cetuximab, an inhibitor of EGF receptor binding and signaling, reduces the kidney levels of anti-ENaCγ and anti-phosphothreonine immunoreactive proteins and raises the BP of salt-loaded mice (19). The physiological significance of the above studies was substantiated by the demonstration that, cetuximab-treated salt-loaded hypertensive mice show reductions in ERK1/2 phosphorylation and in the levels of anti-phosphothreonine immunoreactive proteins in their CDs (19), suggesting reductions in inhibitory ENaCγ threonine phosphorylation. Importantly, a mechanistic commonality between the inhibitory effects of EGF and EETs on ENaC is indicated by the fact that inhibition of EGF receptor signaling (19) or disruption of the renal *Cyp2c44* epoxygenase leads to comparable effects on ENaC activity and systemic BP. Based on these and published studies (19, 21, 23, 26), as well as similarities between EETs and EGF as inhibitors of ENaC activity and activators of mitogenic kinase pathways (15–21, 41, 42), we propose that: (*a*) EGF and Cyp2c44 epoxygenase-derived EETs regulate ENaC activity by common ERK1/2-mediated mechanisms and (*b*) impairments in Cyp2c44-mediated ERK1/2 activation and reduced ENaC phosphorylation contribute to the hypertensive phenotype of *Cyp2c44* KO mice. The above mechanism is consistent with the known roles of EETs on ERK1/2 phosphorylation and EGF signaling (41, 42). In summary, these and other studies (15–19) have characterized functional roles for MEK/ERK members of mitogen-activated kinase signaling cascades in renal sodium transport that appear distinct and independent of their more traditional roles on cell proliferation. Finally, the proposal of roles for the Cyp2c44 epoxygenase in the *in vivo* regulation of mitogenic growth factor-ERK1/2-mediated signaling provides a common experimental platform that could explain the roles reported for the enzyme and EETs in channel activity, cell proliferation, angiogenesis, tumorigenesis, and vasodilation (21, 25, 41, 42). Current efforts are directed toward the characterization of the: (*a*) organ generality of the *Cyp2c44* genotype and EETs effects on ERK1/2 activation and (*b*) mechanism(s) of ERK1/2 activation by EETs.

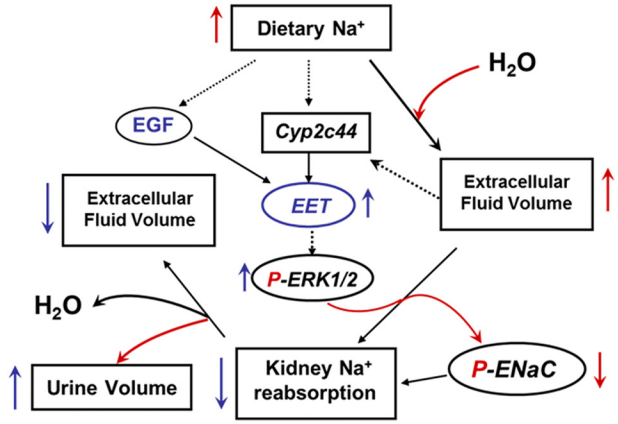

FIGURE 7. **Roles proposed for the epoxygenase the regulation of renal sodium reabsorption and plasma volume.** *Ascending* and *descending arrows* denote increases and decreases in *boxed* parameters, respectively. *Dashed arrows* are used to indicate that the mechanisms by which changes in dietary salt alter EGF signaling and/or Cyp2c44 expression, changes in plasma/extracellular fluid volume regulate Cyp2c44 epoxygenase activity and/or expression, and the EETs regulate the MEK1/2/ERK1/2 pathway remain to be characterized. *Red* and *blue arrows* indicate pro- and antihypertensive effects, respectively.

Based on the results discussed, we would like to extend our previous proposal of the means by which the EETs regulate BP in mice (26) to include effects on the EGF/ERK1/2-mediated inhibition of ENaC. Thus, under conditions of balanced salt intake and excretion, locally generated EETs participate in steady state, nonstimulated ENaC gating and sodium reabsorption. Dietary increases in sodium intake cause compensatory changes in extra cellular fluid volume and rapid and delayed epoxygenase-mediated responses (Fig. 7). The rapid phase involves EGF-stimulated phospholipase-dependent AA release (41, 42) and Cyp2c44 epoxygenase metabolism to EETs (Fig. 7). The delayed phase requires up-regulated Cyp2c44 epoxygenase expression and increases in EET-synthase activity (Fig. 7). Augmented EET levels activate MEK/ERK1/2 kinases resulting in: (*a*) phosphorylation of ENaCβ and ENaCγ, (*b*) channel inactivation and reductions in inward sodium transport, and (*c*)

increases in urine sodium and volume excretion (Fig. 7). Reductions in Cyp2c44 epoxygenase expression or activity increase ENaC-dependent sodium reabsorption and, to maintain plasma sodium levels within physiologically compatible levels, cause attendant changes in extracellular fluid/plasma volume leading to increased systemic BP (Fig. 7) and, ultimately, hypertension. Potential direct effects of salt intake or attendant effects on plasma/extracellular fluid volume on EGF signaling or Cyp2c44 expression and/or activity remain to be characterized, as are mechanisms of MEK/ERK1/2 kinase activation by EETs.

With few exceptions, the molecular basis of the most prevalent forms of human hypertension are yet to be established, and thus, the diagnosis and treatment of this devastating disease remains challenging. This situation arises from the inherent complexity of a disease in which multiple environmental and genetic factors, as well as co-existing conditions, contribute to its multifaceted etiology. The recognition of altered tubular transport in hypertensive *Cyp2c44* KO mice offers new approaches for the understanding of mechanism(s) by which the kidney regulates sodium excretion and blood pressure. Furthermore, the data presented: (*a*) provide an experimental foundation for future studies of the functional roles of the CYP2C8 and CYP2C9 epoxygenases in human hypertension and (*b*) suggest that maneuvers designed to up-regulate kidney CYP2C epoxygenase expression and/or efforts to develop stable EET functional analogs (26, 50) could serve as a basis for the development of novel antihypertensive therapies. In summary, it is expected that these studies will stimulate efforts to develop novel CYP2C/EET-based, antihypertensive drugs and strategies for the early detection and diagnosis of hypertension.

Finally, the recognition of the roles played by the Cyp2c44 epoxygenase in the regulation of ENaC activity, as well as the rapid nature of the inhibitory response elicited by its EET metabolites, introduces a new mechanistic paradigm to account for the regulation of this channel and suggests that genetically determined and/or environmentally induced alterations in the expression and/or activities of the human functional homologues of Cyp2c44 (CYP2C8 and/or CYP2C9) (51) could play a role in the pathophysiology of human hypertension. This is of relevance because several drugs in current clinical use are metabolized by human CYP2C8 and/or CYP2C9 (51) with yet undetermined effects on the regulation and/or epoxygenase activity of these enzymes. It is therefore of importance that the current methods for drug evaluation take into consideration the potential physiological and/or pathophysiological consequences of interfering with the activity and/or expression of P450s involved in endogenous metabolic pathways. This and other published studies (21, 25, 50) should influence current views of the roles played by the P450 enzyme system from that of vehicles for drug disposition and/or activation to that of active participants in the biosynthesis of physiologically important mediators of cell and organ function.

Acknowledgments—We are thankful to Fernando Elijovich MD. for suggestions and helpful comments. The contributions of the Vanderbilt University Mass Spectrometry Center and Small Animal Physiology Core to these studies are also gratefully acknowledged.

REFERENCES

1. Crews,D. C., Plantinga, L. C., Miller, E. R., 3rd, Saran, R., Hedgeman, E., Saydah, S. H., Williams, D. E., Powe, N. R., and Centers for Disease Control and Prevention Chronic Kidney Disease Surveillance Team (2010) Prevalence of chronic kidney disease in persons with undiagnosed prehypertension in the United States. *Hypertension* **55,** 1102–1109
2. Mensah, G. A., Croft, J. B., and Giles, W. H., (2002) The heart, kidney, and brain as target organs in hypertension. *Cardiol. Clin.* **20,** 225–247
3. Lifton, R. P., Gharavi, A. G., and Geller, D. S. (2001) Molecular mechanisms of human hypertension. *Cell* **104,** 545–556
4. Munroe, P. B., Barnes, M. R., and Caulfield, M. J. (2013) Advances in blood pressure genomics. *Circ. Res.* **112,** 1365–1379
5. Pratt, J. H. (2005) Central role for ENaC in the development of hypertension. *J. Am. Soc. Nephrol.* **16,** 3154–3159
6. Rossier, B. C., and Schild, L. (2008) Epithelial sodium channel. Mendelian versus essential hypertension. *Hypertension* **52,** 595–600
7. Hamm, L. L., Feng, Z., and Hering-Smith, K. S. (2010) Regulation of sodium transport by ENaC in the kidney. *Curr. Opin. Nephrol. Hypertens.* **19,** 98–105
8. Canessa, C. M., Schild, L., Buell, G., Thorens, B., Gautschi, I., Horisberger, J. D., and Rossier, B. C. (1994) Amiloride-sensitive epithelial Na^+ channel is made of three homologous subunits. *Nature* **367,** 463–467
9. Snyder, P. M. (2002) The epithelial sodium channel, Cell surface insertion and retrieval in Na^+ homeostasis and hypertension. *Endocr. Rev.* **23,** 258–275
10. Schild, L. (1996) The ENaC channel as the primary determinant of two human diseases, Liddle syndrome and pseudohypo- aldosteronism. *Nephrologie* **17,** 395–400
11. Warnock, D. G. (2001) Liddle syndrome, Genetics and mechanism of Na^+ channel defects. *Am. J. Med. Sci.* **322,** 302–307
12. Chang, S. S., Grunder, S., Hanukoglu, A., Rösler, A., Mathew, P. M., Hanukoglu, I., Schild, L., Lu, Y., Shimkets, R. A., Nelson-Williams, C., Rossier, B. C., and Lifton, R. P. (1996) Mutations in the epithelial sodium channel cause salt wasting with hyperkalaemic acidosis, pseudohypoaldosteronism type 1. *Nat. Genet.* **12,** 248–253
13. Masilamani, S., Kim, G. H., Mitchell, C., Wade, J. B., and Knepper, M. A. (1999) Aldosterone-mediated regulation of ENaC α, β, and γ subunit proteins in rat kidney. *J. Clin. Invest.* **104,** R19–R23
14. Zhang, Y. H., Alvarez de la Rosa, D., Canessa, C. M., and Hayslett, J. P. (2005) Insulin-induced phosphorylation of ENaC correlates with increased sodium channel function in A6 cells. *Am. J. Physiol. Cell Physiol.* **288,** C141–C147
15. Vehaskari, V. M., Hering-Smith, K. S., Moskowitz, D. W., Weiner, I. D., and Hamm, L. L. (1989) Effect of epidermal growth factor on sodium transport in the cortical collecting tubule. *Am. J. Physiol.* **256,** F803–F809
16. Shen, J. P., and Cotton, C. U. (2003) Epidermal growth factor inhibits amiloride-sensitive sodium absorption in renal collecting duct cells. *Am. J. Physiol. Renal Physiol.* **284,** F57–F64
17. Shi, H., Asher, C., Chigaev, A., Yung, Y., Reuveny, E., Seger, R., and Garty, H. (2002) Interactions of β and ENaC with Nedd4 can be facilitated by an ERK-mediated phosphorylation. *J. Biol. Chem.* **277,** 13539–13547
18. Falin, R. A., and Cotton, C. U. (2007) Acute downregulation of ENaC by EGF involves the PY motif and putative ERK phosphorylation site. *J. Gen. Physiol.* **130,** 313–328
19. Pidkovka, N., Rao, R., Mei, S., Gong, Y., Harris, R. C., Wang, W. H., and Capdevila, J. H. (2013) Epoxyeicosatrienoic acids (EETs) regulate epithelial sodium channel activity by extracellular signal-regulated kinase 1/2 (ERK1/2)-mediated phosphorylation. *J. Biol. Chem.* **288,** 5223–5231
20. Capdevila, J. H., and Falck, J. R. (2002) Biochemical and molecular properties of the cytochrome P450 arachidonic acid monooxygenases. *Prostaglandins Other Lipid Mediat.* **68–69,** 325–344
21. Capdevila, J. H. (2007) Regulation of ion transport and blood pressure by cytochrome P450 monooxygenases. *Curr. Opin. Nephrol. Hypertens.* **16,** 465–470
22. Spector, A. A. (2009) Arachidonic acid cytochrome P450 epoxygenase pathway. *J. Lipid Res.* **50,** S52–S56
23. Wei, Y., Lin, D.-H., Kemp, R., Yaddanapudi, G. S., Nasjletti, A., Falck, J. R.,

and Wang, W. H. (2004) Arachidonic acid inhibits epithelial Na channel via cytochrome P450 (CYP) epoxygenase-dependent metabolic pathways. *J. Gen. Physiol.* **124,** 719–727
24. Sun, P., Lin, D. H., Yue, P., Jiang, H., Gotlinger, K. H., Schwartzman, M. L., Falck, J. R., Goli, M., and Wang, W. H. (2010) High potassium intake enhances the inhibitory effect of 11,12-EET on ENaC. *J. Am. Soc. Nephrol.* **21,** 1667–1677
25. Pozzi, A., Popescu, V., Yang, S., Mei, S., Shi, M., Puolitaival, S. M., Caprioli, R. M., and Capdevila, J. H. (2010) The anti-tumorigenic properties of the peroxisomal proliferator-activated receptor α are arachidonic acid epoxygenase mediated. *J. Biol. Chem.* **285,** 12840–12850
26. Nakagawa, K., Holla, V. R., Wei, Y., Wang, W. H., Gatica, A., Wei, S., Mei, S., Miller, C. M., Cha, D. R., Price, E., Jr., Zent, R., Pozzi, A., Breyer, M. D., Guan, Y., Falck, J. R., Waterman, M. R., and Capdevila, J. H. (2006) Salt-sensitive hypertension is associated with dysfunctional *Cyp4a10* gene and kidney epithelial sodium channel. *J. Clin. Invest.* **116,** 1696–1702
27. Manhiani, M., Quigley, J. E., Knight, S. F., Tasoobshirazi, S., Moore, T., Brands, M. W., Hammock, B. D., and Imig, J. D. (2009) Soluble epoxide hydrolase gene deletion attenuates renal injury and inflammation in DOCA-salt hypertension. *Am. J. Physiol. Renal Physiol.* **297,** F740–F748
28. Guan, Y., Hao, C., Cha, D. R., Rao, R., Lu, W., Kohan, D. E., Magnuson, M. A., Redha, R.,Zhang, Y., and Breyer, M. D. (2005) PPARγ regulates systemic fluid volume by activating sodium absorption in the collecting duct. *Nat. Med.* **11,** 861–866
29. Capdevila, J. H., Dishman, E., Karara, A., and Falck, J. R. (1991) Cytochrome P450 arachidonic acid epoxygenase. Stereochemical characterization of epoxyeicosatrienoic acids. *Methods Enzymol.* **206,** 441–453
30. Rossier, B. C., and Stutts, M. J. (2009) Activation of the epithelial sodium channel (ENaC) by serine proteases. *Annu. Rev. Physiol.* **71,** 361–379
31. Holthöfer, H., Schulte, B. A., and Spicer, S. S. (1987) Expression of binding sites for *Dolichos biflorus* agglutinin at the apical aspect of collecting duct cells in rat kidney. *Cell Tissue Res.* **249,** 481–485
32. DeLozier, T. C., Tsao, C. C., Coulter S. J., Foley, J., Bradbury, J. A., Zeldin, D. C., and Goldstein, J. A. (2004) CYP2C44, a new murine CYP2C that metabolizes arachidonic acid to unique stereospecific products. *J. Pharmacol. Exp. Ther.* **310,** 845–854
33. Makita, K., Takahashi, K., Karara, A., Jacobson, H. R., Falck, J. R., and Capdevila, J. H. (1994) Experimental and/or genetically controlled alterations of the renal microsomal cytochrome P450 epoxygenase induce hypertension in rats fed a high salt diet. *J. Clin. Invest.* **94,** 2414–2420
34. Tsao, C. C., Coulter, S. J., Chien, A., Luo, G., Clayton, N. P., Maronpot, R., Goldstein, J. A., and Zeldin, D. C. (2001) Identification and localization of five CYP2Cs in murine extrahepatic tissues and their metabolism of arachidonic acid to regio- and stereoselective products. *J. Pharmacol. Exp. Ther.* **299,** 39–47
35. Sun, P., Antoun, J., Lin, D.-H., Yue, P., Gotlinger, K. H., Capdevila, J., and Wang, W. H. (2012) Cyp2c44 epoxygenase is essential for preventing the renal sodium absorption during increasing dietary potassium intake. *Hypertension* **59,** 339–347
36. Roman, R. J., and Osborn, J. L. (1987) Renal function and sodium balance in conscious Dahl S and R rats. *Am. J. Physiol.* **252,** R833–R841
37. Möller, B., and Hansell, P. (1995) Sodium and dopamine excretion in prehypertensive Dahl rats during severe hypervolaemia. *Acta Physiol. Scand.* **155,** 165–171
38. Intersalt Cooperative Research Group (1988) Intersalt, an international study of electrolyte excretion and blood pressure. Results for 24 hour urinary sodium and potassium excretion. *BMJ* **297,** 319–328
39. Jacobson, H. R., Corona, S., Capdevila, J., Chacos, N., Manna, S., Womack, A., and Falck, J. R. (1984) Effects of epoxyeicosatrienoic acids on ion transport in the rabbit cortical collecting tubule. In *Prostaglandins and Membrane Ion Transport*, pp. 311–318, Raven Press, New York
40. Pavlov, T. S., Ilatovskaya, D. V., Levchenko, V., Mattson, D. L., Roman, R. J., and Staruschenko, A. (2011) Effects of cytochrome P450 metabolites of arachidonic acid on the epithelial sodium channel (ENaC). *Am. J. Physiol. Renal. Physiol.* **301,** F672–F681
41. Chen, J. K., Wang, D.-W., Falck, J. R., Capdevila, J., and Harris, R. C. (1999) Transfection of an active cytochrome P450 arachidonic acid epoxygenase indicated that 14,15-epoxyeicosatrienoic acid functions as an intracellular second messenger in response to epidermal growth factor. *J. Biol. Chem.* **274,** 4764–4769
42. Chen, J. K., Capdevila, J., and Harris, R. C. (2002) Heparin-binding EGF-like growth factor mediates the biological effects of P450 arachidonate epoxygenase metabolites in epithelial cells. *Proc. Natl. Acad. Sci. U.S.A.* **99,** 6029–6034
43. Hu, J. C., Bengrine, A., Lis, A., and Awayda, M. S. (2009) Alternative mechanisms of activation of the epithelial Na^+ channel by cleavage. *J. Biol. Chem.* **284,** 36334–36345
44. Ergonul, Z., Frindt, G., and Palmer, L. G. (2006) Regulation of maturation and processing of ENaC subunits in the rat kidney. *Am. J. Physiol. Renal Physiol.* **291,** F683–F693
45. Butterworth, M. B., Weisz, O. A., and Johnson, J. P. (2008) Some assembly required, Putting the epithelial sodium channel together. *J. Biol. Chem.* **283,** 35305–35309
46. Butterworth, M. B., Edinger, R. S., Frizzell, R. A., and Johnson, J. P. (2009) Regulation of epithelial sodium channel by membrane trafficking. *Am. J. Physiol. Renal Physiol.* **296,** F10–F24
47. Thomas, C. P., and Itani, O. A. (2004) New insights into epithelial sodium channel function in the kidney, site of action, regulation by ubiquitin ligases, serum- and glucocorticoid-inducible kinases and proteolysis. *Curr. Opin. Nephrol. Hypertens.* **13,** 541–548
48. Fejes-Tóth, G., Frindt, G., Náray-Fejes-Tóth, A., and Palmer L. G. (2008) Epithelial Na^+ channel activation and processing in mice lacking SGK1. *Am. J. Physiol. Renal Physiol.* **294,** F1298–F1305
49. Pochynyuk, O., Bugaj, V., and Stockand, J. D. (2008) Physiological regulation of the epithelial sodium channel by phosphatidylinositides. *Curr. Opin. Nephrol. Hypertens.* **17,** 533–540
50. Imig, J. D., Elmarakby, A., Nithipatikom, K., Wei, S., Capdevila, J. H., Tuniki, V. R., Sangras, B., Anjaiah, S., Manthati, V. L., SudarshanReddy, D., and Falck, J. R. (2010) Development of epoxyeicosatrienoic acid analogs with *in vivo* anti-hypertensive actions. *Front. Physiol.* **1,** 157
51. Guengerich, F. P. (2006) Cytochrome P450s and other enzymes in drug metabolism and toxicity. *AAPS J.* **8,** E101–E111